

Point-contact spectroscopy of electron-phonon interaction in superconductors

N. L. Bobrov *, A. V. Khotkevich, G. V. Kamarchuk, and P. N. Chubov

B.I. Verkin Institute for Low Temperature Physics and Engineering,

of the National Academy of Sciences of Ukraine, prospekt Lenina, 47, Kharkov 61103, Ukraine

(Dated: May 28, 2014; Published Fiz. Nizk. Temp. 2014, **40**, p.280(Low Temp. Phys. 2014, **40**, p.215))

The possibility to reconstruct the electron-phonon interaction (EPI) function was demonstrated for $S - c - N$ and $S - c - S$ point contacts using the superconducting inelastic contribution to the excess current caused by Andreev reflection processes. Superconductors with both weak (Sn, Al) and strong (Pb, In) EPI were considered. It was shown that in the latter case it is necessary to account for the elastic component of current which is related to the frequency dependence of the superconducting energy gap arising due to electron-phonon renormalization of the energy spectrum of the superconductor.

PACS numbers: 71.38.-k, 73.40.Jn, 74.25.Kc, 74.45.+c, 74.50.+r.

I. INTRODUCTION

The significant progress recently made in the development of new superconducting materials stirred a growing interest in determining their key parameters. One of the most important characteristics that allow analyzing the superconductor behavior for the synthesis of new superconducting compounds is the electron-phonon interaction (EPI) function. One of the major techniques employed to determine the EPI function is Yanson's point-contact (PC) spectroscopy. This method has worked well for measuring nonlinearities of current-voltage characteristics (CVC) in the point contacts consisting of metals and compounds in the normal state^{1,2}. On the other hand, for many superconductors it is very difficult to realize the ballistic regime of current flow during their transition to normal state, which is necessary for providing the spectral mode of operation of a point-contact in Yanson's point-contact spectroscopy. This problem is most pronounced when the compounds belonging to the new classes of superconducting materials are studied. The pointcontact studies of such materials often have to deal with a much distorted surface layer, which limits the possibility of determining the EPI parameters. An effective solution to this problem is to use the point-contact characteristics measured in the superconducting state³.

II. BASIC THEORETICAL CONCEPTIONS

A. Inelastic contribution

The theory of inelastic spectroscopy of the EPI in a superconductor considers ballistic point contacts with the dimensions d smaller than all characteristic lengths⁴⁻⁶: $d \ll \xi(0)$, l_i , v_F/ω_D , where $\xi(0)$ is the superconducting coherence length, l_i is the scattering length on impurities,

$l_\epsilon \sim v_F/\omega_D$ is the energy mean free path at the Debye energy.

We should emphasize an important point: despite the fact that most of the nonequilibrium phonons are generated in the banks of the contact and any scattering process of the Andreev electrons on nonequilibrium phonons is effective, the existing theories consider only scattering in the region of maximum concentration of nonequilibrium phonons since the probability of their re-absorption by electrons depends on the concentration of phonons. This region corresponds to the highest current density and has a size, as also in the case of Yanson's point-contact spectroscopy, of the order of the contact diameter⁷.

The first publication³ on the reconstruction of EPI functions from the spectra of superconducting point contacts has addressed the cases that, to a certain extent, go beyond the predictions of the theory of inelastic spectroscopy of EPI in superconductors⁴⁻⁶. In these cases, scattering in the banks played an important role in the formation of nonlinearities in such point contacts. However, the contacts which satisfy the theoretical model to the fullest extent have not been considered. In this paper, we will fill this gap and also consider the point contacts in which the elastic contribution to electronphonon scattering should be taken into account.

At the heart of the inelastic point contact spectroscopy of superconductors lies the study of nonlinear current-voltage characteristics of the contacts arising due to the inelastic scattering of nonequilibrium phonons on electrons undergoing Andreev reflection.

In Yanson's point contact spectroscopy the EPI function is

$$G_{pc}(eV) = -\frac{3R_0\hbar v_F}{32ed} \cdot \frac{d^2 I}{dV^2},$$

i.e., it is proportional to the second derivative of the current-voltage characteristic.⁷ At the same time in the inelastic PC spectroscopy of superconductors,⁴⁻⁶ the EPI function is proportional to the first derivative of the excess current (the difference between the current-voltage characteristics in the normal and superconducting states at the same voltage). For $S - c - S$ contacts, the following

*Email address: bobrov@ilt.kharkov.ua

expression has been obtained⁴:

$$\frac{dI_{exc}}{dV} = -\frac{64}{3R} \left(\frac{\Delta L}{\hbar v} \right) \left[G^N(\omega) + \frac{1}{4} G^S(\omega) \right] \quad \omega = eV/\hbar \quad (1)$$

$G^N(\omega)$ is the PC EPI function identical to that of the point contact in the normal state, $G^S(\omega)$ is the superconducting PC EPI function different from $G^N(\omega)$ by a form factor. In contrast to the normal form factor, which determines the contribution to the current due to electron-phonon collisions accompanied by a change in the z -component of the electron velocity, in the case of the superconducting form factor which is included in $G^S(\omega)$, it is the electron-phonon collisions associated with Andreev reflection processes in the contact region, i.e., conversion of quasi-electron into quasi-hole excitations, that contribute to the current. The relative magnitude of the phonon contribution to the excess current is of the order of $d \cdot \omega_D / v_F$, for $eV \sim \omega_D$, i.e., it is small if the condition $d \ll v_F / \omega_D$ is fulfilled.

An analogous expression for $S-c-N$ contacts is⁵

$$\begin{aligned} & \left. \frac{1}{R(V)} - \frac{1}{R(V)} \right|_{\Delta=0} = \\ & = -\frac{32d\Delta}{3R\hbar} \left[\frac{1}{v_F^{(1)}} G_1(\omega) + \frac{1}{v_F^{(2)}} G_2(\omega) \right] \end{aligned} \quad (2)$$

For the second derivative of the CVC in $S-c-N$ point contacts, the following expression has been obtained:

$$\frac{1}{R} \frac{dR}{dV} = \frac{16ed}{3\hbar} \sum_{a=1,2} \frac{1}{v_F^{(a)}} \int_0^\infty \frac{d\omega}{\Delta} S\left(\frac{\omega - eV}{\Delta}\right) G_a(\omega) \quad (3)$$

$G_a(\omega)$ are the EPI functions for the normal and superconducting metals forming the heterojunction, $S(x)$ is the smearing factor,

$$S(x) = \theta(x-1) \frac{2(x - \sqrt{x^2 - 1})^2}{\sqrt{x^2 - 1}}, \quad (4)$$

where $\theta(x)$ is the Heaviside theta-function. Thus, for $T \rightarrow 0$, the resolution is determined by the value of Δ . From expression (3), given the relation between the derivative of CVC and the PC EPI function, it can be written as

$$\tilde{g}_{pc}^S = \int_0^\infty \frac{d\omega}{\Delta} S\left(\frac{\omega - eV}{\Delta}\right) g_{pc}^N(\omega) \quad (5)$$

As a model $g_{pc}^N(\omega)$, we will take the EPI function of Cu-Sn heterojunction reconstructed from its spectrum in the normal state.

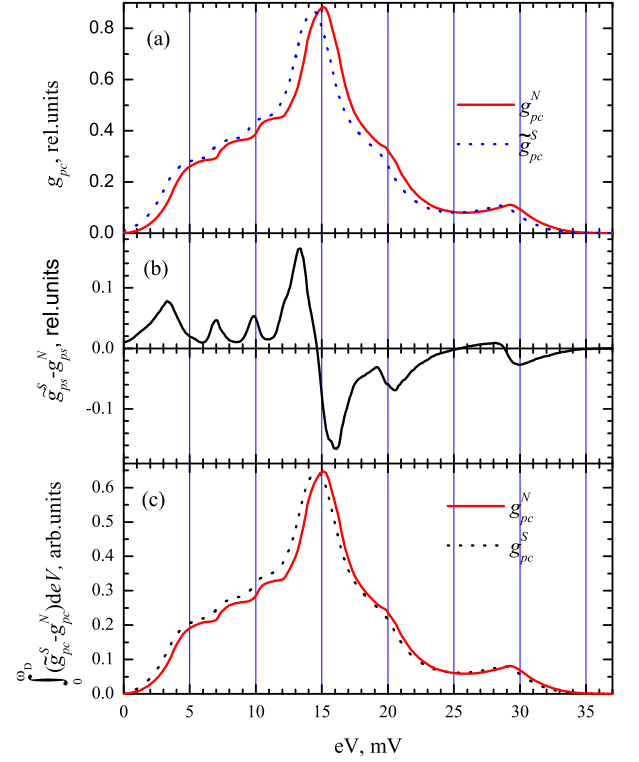


FIG. 1: g_{PC}^N is the EPI function of Sn-Cu point contact reconstructed from the spectrum shown in Fig.2 \tilde{g}_{PC}^S is the theoretically predicted point-contact EPI function upon transition into the superconducting state (Eq.(5), see text for more detail) (a); difference curve (b); integral of the difference curve, point-contact EPI function obtained from the first derivative of the excess current \tilde{g}_{PC}^S in comparison with g_{PC}^N . For convenience of comparison, the maximum values of the curves are set the same.

The calculation results obtained using (5) in Fig. 1. In comparison to the original N -curve, the S -curve exhibits a shift of the EPI maxima towards lower energies by the magnitude of the gap Δ . Moreover, its amplitude is somewhat smaller than the amplitude of the initial curve due to an additional broadening by the smearing factor S , Eq.(4). As already mentioned, in the superconducting state, the EPI spectrum should appear in the first derivative of the excess current. Indeed, if we subtract the initial N -curve from the S -curve, we obtain the $S-N$ curve: $\tilde{g}_{pc}^S - g_{pc}^N$. As follows from Eq.(2), the EPI function can be reconstructed from the first derivative of the excess current:

$$g_{pc}^S(eV) = \frac{1}{\Delta} \int_0^{eV} [\tilde{g}_{pc}^S(\omega) - g_{pc}^N(\omega)] d\omega \quad (6)$$

It should be emphasized that \tilde{g}_{pc}^S and g_{pc}^S are different functions. The former one, given by Eq.(5), is proportional to the second derivative of the CVC and reflects the transformation of the spectrum (broadening and the

shift of the phonon peaks) upon transition of the heterojunction into the superconducting state. The latter one, given by Eq.(6), see also Eq.(2), is proportional to the first derivative of the excess current and does not contain any additional broadening. The position of the phonon maxima in the $g_{pc}^S(eV)$ is intermediate between \tilde{g}_{pc}^S and g_{pc}^N . Note that for $S - c - S$ contacts, the position of maxima in the EPI function reconstructed from the first derivative of the excess current match that for the normal condition.

B. Elastic contribution

The CVC of a point contact in which one or both electrodes contain a superconductor with strong EPI comprises, along with the above nonlinearities, an additional **elastic** component of the current related to the frequency dependence of the superconducting energy gap. This additional nonlinearity arises due to the electron-phonon renormalization of the energy spectrum of the superconductor and is manifested as *differential conductance maxima* in the region of characteristic phonon energies in the first derivative of the excess current, which are shifted to higher energies by the magnitude of the superconducting energy gap⁸.

Equation (7), which describes the first derivative of the CVC in a point contact with direct conductivity, differs from the corresponding expression (8) for a tunnel junction,⁸

$$\left(\frac{dI}{dV}\right)_{S-c-N} = \frac{1}{R_0} \left\{ 1 + \left| \frac{\Delta(\varepsilon)}{\varepsilon + \sqrt{\varepsilon^2 - \Delta^2(\varepsilon)}} \right|_{\varepsilon=eV}^2 \right\} \quad (7)$$

$$\left(\frac{dI}{dV}\right)_{S-I-N} = \frac{1}{R_0} Re \left\{ \frac{\varepsilon}{\sqrt{\varepsilon^2 - \Delta^2(\varepsilon)}} \right\}_{\varepsilon=eV} \quad (8)$$

This difference is due to Andreev reflection processes leading to an excessive current in the region $eV \gg \Delta_0$.

Note that, unfortunately, the above equations do not cover the most frequently encountered experimental situation- point contacts with arbitrary transparency of the tunnel barrier between the electrodes. In this respect, the situation is similar to the attempts to determine the superconducting energy gap prior to the BTK theory (Blonder, Tinkham, and Klapwijk)⁹, which has provided a method for determining the gap that takes into account an arbitrary barrier transparency. It should be noted that for inelastic superconducting spectroscopy this gap has been filled by Ref.⁶.

Obviously, for point contacts with low barrier transparency, it is the elastic contribution that is predominant due to the suppression of the excess current. It has been noted in Ref.⁸ that for ballistic contacts, CVC nonlinearities of elastic origin may be comparable with the inelastic

TABLE I: Estimated elastic spectral contribution normalized by that of Pb, δ_{rel} , superconducting gap and transition temperature for several superconductors (SC).

SC	Pb	In	Sn	Ta	Al	NbSe ₂	MgB ₂
δ_{rel}	1	0.21	0.078	0.063	0.00168	0.023	0.24
Δ_0, mV	1.365	0.525	0.575	0.7	0.17	1.07÷2.48	1.8÷7.4
T_C, K	7.2	3.415	3.722	4.47	1.181	7.2	39

contributions in point contacts. For the point contacts with direct conductivity or high barrier transparency, the ratio between the elastic and inelastic contributions is determined by the parameters of the superconductor. As follows from Ref.¹⁰, the expected elastic contribution to the spectrum is proportional to $\sim (T_C/\theta_D)^2$, where θ_D is the Debye temperature. Table 1 shows the elastic contributions for a number of superconductors normalized by that of lead δ_{rel} , which have been studied in the previous publication³ and in the present paper. The data from Ref.¹⁰ were taken as a basis. We normalized the data by the elastic contribution of lead since it has the highest elastic contribution among the considered superconductors. Table 1 also shows the energy gap and superconducting transition temperature.

Recall that for $S - c - N$ point contacts, the **inelastic** superconducting contribution to the spectrum manifests itself as *differential resistance maxima* in the first derivative of the excess current, which are shifted to lower energies by the distance of the order of the gap. On the other hand, there is no such shift for $S - c - S$ point contacts. Therefore, *these contributions oppose each other* and, if their magnitude is similar, might attenuate each other. Since the inelastic contribution is proportional to the magnitude of the excess current, i.e., Δ , and the elastic contribution is proportional to $(\Delta/E)^2$ (Ref.¹⁰) (see also Eq.(7)), starting from a certain value of Δ , the elastic contribution dominates.

It can be expected that the positions of the maxima in the EPI functions reconstructed from $S - c - S$ and $S - c - N$ point contacts, as well as that for weakly coupled superconductors, will be different.

Both for tunneling and point contacts with direct conductivity, the elastic contribution to the spectrum does not explicitly contain the EPI function $g(\omega)$. However, it can be reconstructed by inverting the Eliashberg equations (similar to the case of Rowell-McMillan's elastic tunneling spectroscopy¹¹).

III. RECONSTRUCTION OF THE EPI FUNCTIONS

A. Sn-based point contacts

Fig. 2 (a) shows the spectra of Sn-Cu point contacts in the normal and superconducting states.¹² Markedly lower level of background in the superconducting spec-

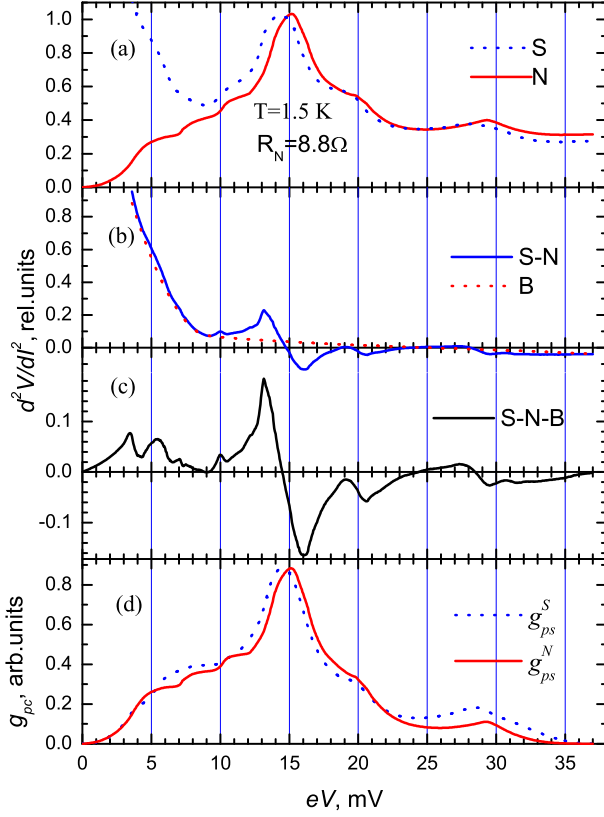


FIG. 2: EPI spectra of Sn-Cu point contact in the normal and superconducting states. Superconductivity is suppressed by a magnetic field (a); the difference between the spectra in the superconducting and normal states and the estimated background curve (b); difference curve (after subtracting the background B) (c); point-contact EPI function reconstructed by integrating the curve in panel (c) versus the EPI function of the normal state (d).

trum and the presence of the gap peak in the region of low energies requires, similar to the previous work,³ that the background B is subtracted from the difference curve $S - N$. The difference curve with the background subtracted, $S - N - B$, is very close to the theoretically calculated curve $\tilde{g}_{pc}^S - g_{pc}^N$ in Fig. 1. Finally, the lower part of the figure shows a comparison of the PC EPI function reconstructed from the spectrum in the normal state (curve g_{pc}^N) and the EPI function reconstructed from the superconducting contribution to the spectrum (curve g_{pc}^S). For convenience of comparison, the curves are plotted with equalized amplitude. There is excellent agreement with the theoretically predicted behavior of the superconducting EPI function—the shift of the maxima to lower energies by the distance of the order of the gap. A slight mismatch in the shape of the curve reconstructed from the experimental data as compared to the calculated EPI function in the region of large displacements can be related to certain arbitrariness in defining the background or an increasing contribution from the peripheral regions of the point contact. The latter can

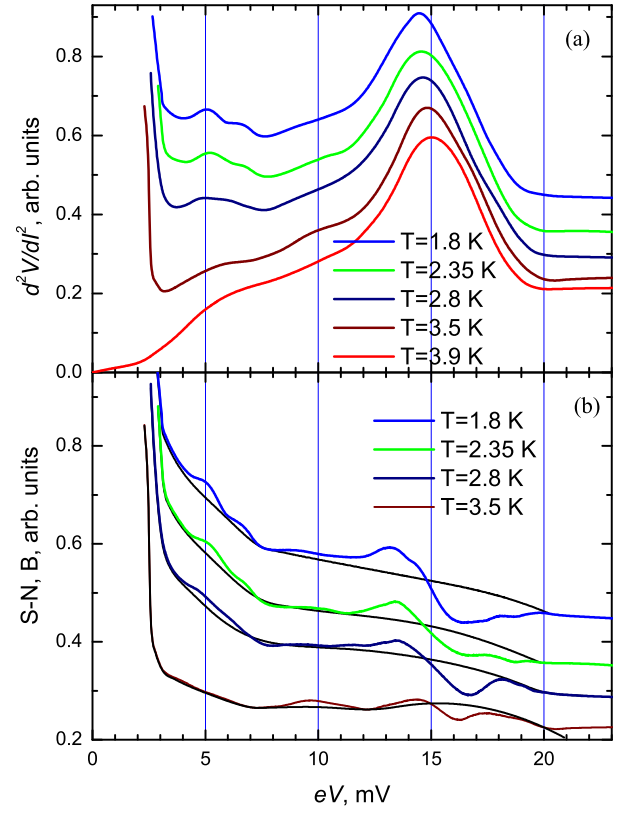


FIG. 3: Point-contact spectra of Sn in the normal and superconducting state, adopted from Ref.¹³. $H = 0$ (a). Superconducting contribution to the spectrum at different temperatures and the estimated background curves (b). $T = 1.8K$: $T/T_C = 0.48$, $\Delta = 0.96\Delta_0$; $T = 2.35K$: $T/T_C = 0.63$, $\Delta = 0.89\Delta_0$, $T = 2.8K$: $T/T_C = 0.75$, $\Delta = 0.78\Delta_0$, $T = 3.5K$: $T/T_C = 0.94$, $\Delta = 0.41\Delta_0$.

occur due to the increasing concentration of nonequilibrium phonons in these regions caused by decreasing the electron energy relaxation length in the vicinity of the Debye energy.

As already noted, in the case of $S - c - S$ contact, the EPI function reconstructed from the first derivative of the excess current exhibits the same position of the maxima as the EPI function of the normal state. Although an expression similar to Eq.(3) describing the transformation of the second derivative of CVC upon the transition of electrodes into the S -state has not been given in Ref.⁴, from the similarity of the expressions (1) and (2), we can assume that the algorithm used for $S - c - N$ point contacts can be employed here as well. Fig.3(a) shows a set of the second derivatives of CVC obtained in the normal and superconducting states,¹³ and Fig.3(b) displays the spectral contribution associated with superconductivity as well as the estimated background curves.

Fig.4 shows the difference curves after background subtraction. Despite the fact that, unlike the previous case for the Sn-Cu point contact, the temperatures of the normal and superconducting states are not the same, the

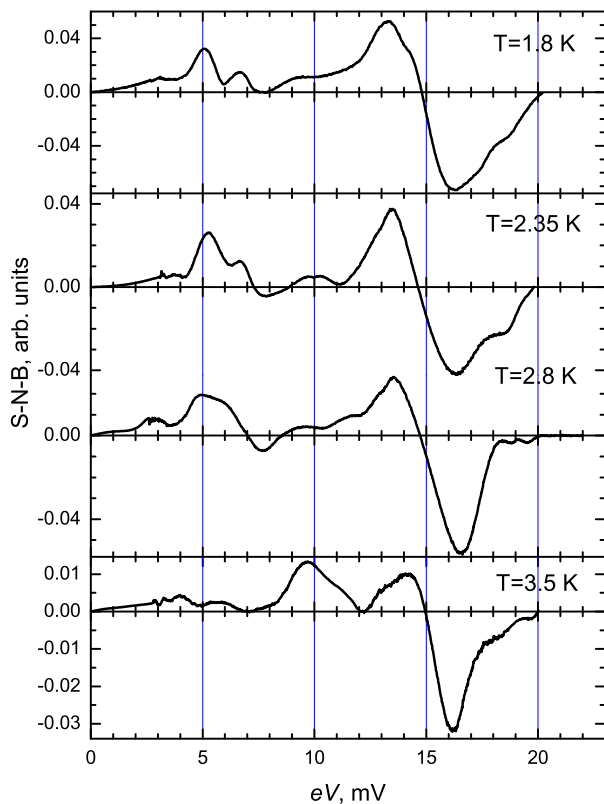


FIG. 4: Superconducting contribution to the point-contact spectra of Sn at different temperatures after subtracting the background curves (Fig.3).

reconstruction of the EPI functions from the superconducting spectral contribution (Fig.5) is quite satisfactory.

Minor variations in the shape of the curves can be easily explained by certain arbitrariness in defining the background. Even for temperatures near T_C , the reconstructed curve matches the normal state spectrum quite satisfactory and the agreement can be further improved by a better choice of the background curve.

B. Al-based point contacts

Aluminum has a relatively low superconducting transition temperature and a small value of the superconducting energy gap (Table 1). This means a small superconducting contribution to the spectrum. Together with the inevitable inaccuracies arising when scanned experimental curves are digitized, this leads to a relatively low accuracy of the difference curve obtained. Nevertheless, the curves shown in Fig.6 (similar to the curves published in Ref.¹⁴) demonstrate that the normal and superconducting EPI functions match each other sufficiently well.

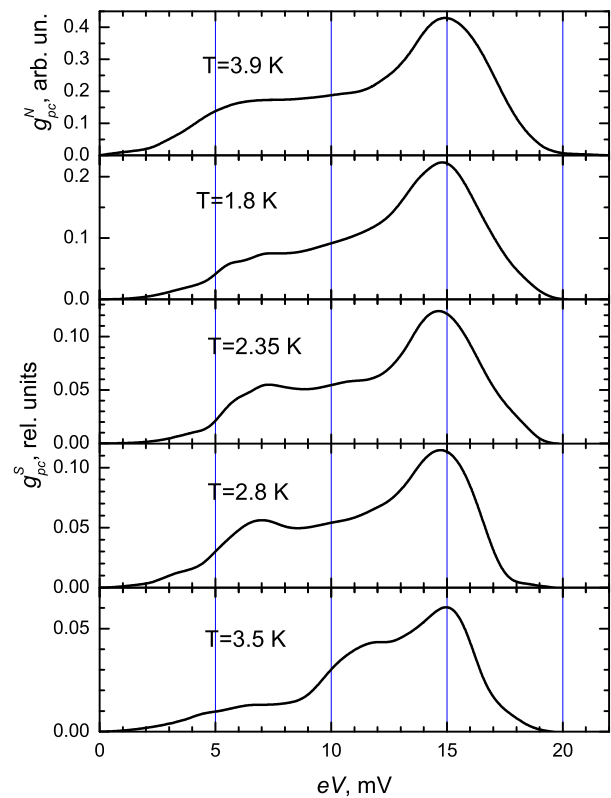


FIG. 5: Point-contact EPI functions of Sn, which were reconstructed from the difference curves shown in Fig.4.

C. Pb-based point contacts

Lead has highest elastic contribution of known superconductors (Table 1). In Ref.¹⁵, the second derivatives of CVC for Pb-Ru heterojunctions have been measured in both the superconducting S and normal N states (Fig.7).

The EPI spectrum of ruthenium does not overlap in energy with the spectrum of lead and therefore was not taken into account. The intensity of the reduced spectrum of lead is close to the maximum for a symmetric heterojunction (0.4 of the maximum intensity for a homojunction). Full contribution to the spectrum associated with superconductivity (the difference curve $S - N$), shown in Fig.7(b), is quite different from similar contributions to the spectrum in metals with weak electron-phonon interaction and does not allow to restore the EPI function using the methods previously employed, in particular, subtraction of a smooth background. The figure also shows the second derivative $d^2V/dI^2(eV)$ of the elastic superconducting contribution to the spectrum ("theory" curve), which was obtained from the dI/dV dependence found from Eq.(7) by numerical differentiation. When calculating dI/dV , the tables of real and imaginary parts of $\Delta(\varepsilon)$ ¹⁶ obtained from tunneling experiments were used.

Although the calculated second derivative of the elastic contribution ("theory" curve) is similar to the differ-

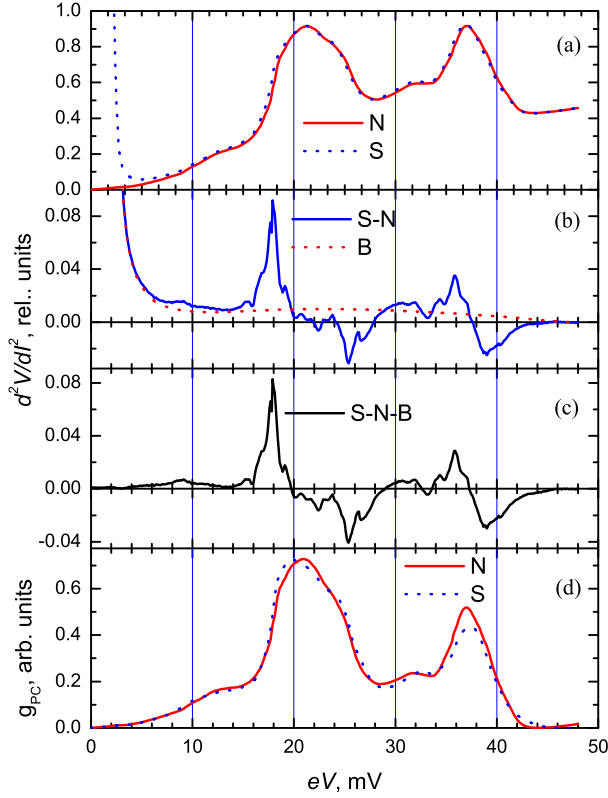


FIG. 6: EPI spectra of an Al-Al point contact in the normal and superconducting states. $T/T_C = 0.68$, $\Delta = 0.85\Delta_0$. Superconductivity is suppressed by a magnetic field (a). The difference between the superconducting and normal spectra and the estimated background curve (b). Difference curve (after background subtraction) (c). Point-contact EPI function reconstructed by integrating the difference curve in panel (c) versus the EPI function of the normal condition (d).

ence curve $S - N$, there are notable differences, especially at high energies. As already mentioned, the elastic superconducting contribution manifests itself as maxima of the differential conductance in the region of characteristic phonon energies in the first derivative of the excess current. However, the difference curve $S - N$ contains not only the elastic contribution, but also inelastic one, and, apparently, in the same way as in the superconductors with weak coupling, also additional nonlinearity which is not accounted by the theory and is what we call a superconducting background. Therefore, to obtain the EPI spectrum by integration, as was done previously, let us try to subtract the background from the difference curve $S - N$ using the same rules as in the case of weakly coupled superconductors. *After background subtraction, the areas under the curve above and below the abscissa should be the same; for energies above the Debye energy, the curve obtained after background subtraction must be zero.*

The obtained background B is shown in Fig.7(b) as a dashed curve, and the resulting curve after background subtraction, $S - N - B$ is displayed in Fig.7(c). Fig.7(d)

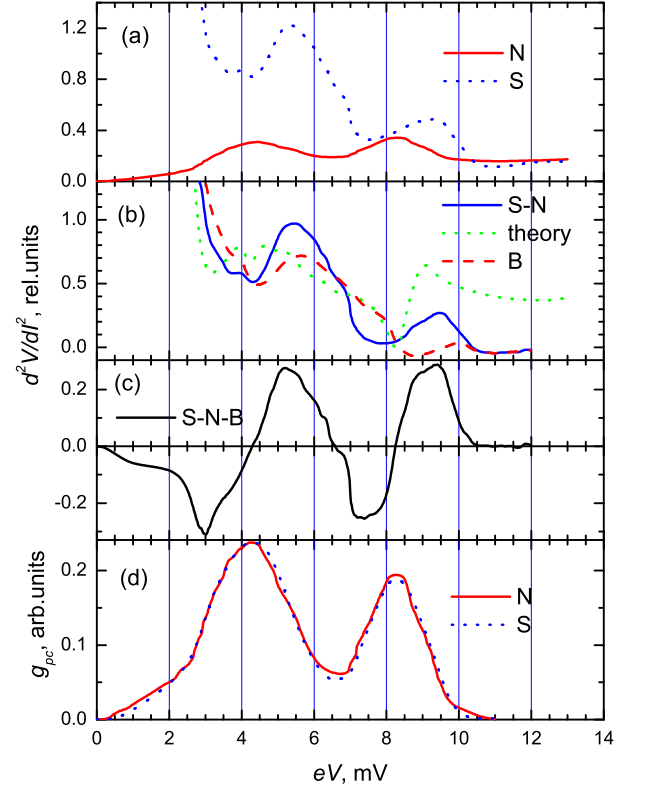


FIG. 7: EPI spectra of a Pb-Ru point contact in the normal and superconducting states. Superconductivity is suppressed by a magnetic field (a). The difference between the superconducting and normal spectra and the estimated background curve. The dashed line shows the theoretically calculated elastic contribution to the spectrum (see text) (b). Difference curve (after background subtraction) (c). Point-contact EPI function reconstructed by integrating the difference curve in panel (c) versus the EPI function of the normal condition (d).

shows the EPI N function reconstructed from the spectrum in the normal state and the EPI S function obtained by integrating the curve $S - N - B$. Here it is necessary to emphasize the following points. First, as follows from the theoretical predictions, the maxima of the function correspond to the maxima of the differential conductance and not to the maxima of resistance as in the case of the superconductors with weak EPI. After integration the curve is inverted. Secondly, the positions of the phonon peaks in the both curves coincide, and there is no shift of the phonon peaks in the restored EPI function for S-c-N point contacts. And finally, the background curve is not smooth and monotonic but is similar in shape to the theoretically calculated elastic contribution marked as "theory". Note that for $S - c - S$ contacts, as discussed below, there is a shift of the phonon maxima in the reconstructed EPI function to higher energies by the distance of the order of Δ .

Fig.8 shows the spectra of a Pb-Pb point contact in the normal and superconducting states¹⁷. The curves

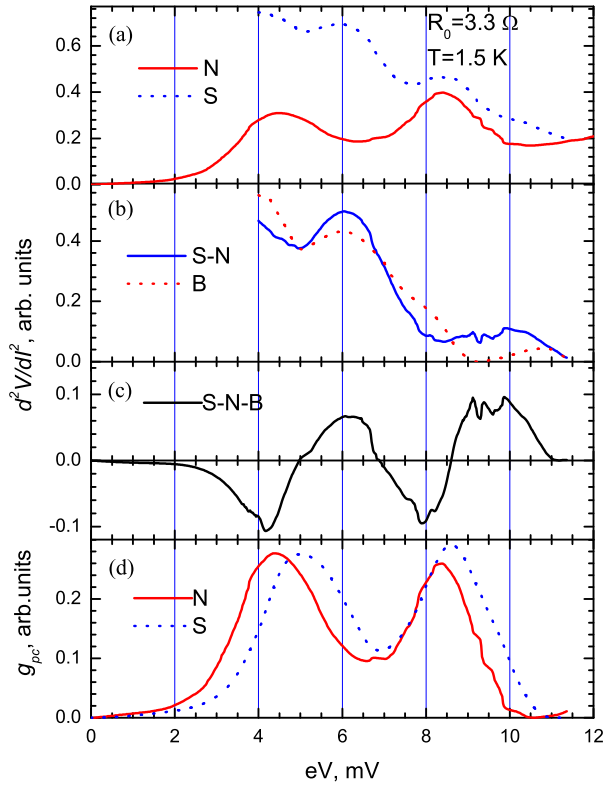


FIG. 8: EPI spectra of a Pb-Pb point contact in the normal and superconducting states. Superconductivity is suppressed by a magnetic field (a). The difference between the superconducting and normal spectra and the estimated background curve (b). Difference curve (after background subtraction) (c). Point-contact EPI function recovered by integrating the curve in panel (c) versus the EPI function of the normal state (g).

were treated similar to the previous case. As anticipated above, the position of the phonon peaks in the EPI function reconstructed from a $S - c - S$ contact differs from that of a $S - c - N$ contact and is shifted toward higher energies by a distance of the order of Δ .

Finally, the data for a Pb-Sn point contact at temperatures above T_C for Sn are shown in Fig. 9.¹⁷ In this case, the tin contribution is considerably higher than that of ruthenium, and it overlaps in energy with the spectrum of lead. Thus it should be necessarily taken into account in data processing. Since this is an $S - c - N$ point contact, there is no shift of the phonon peaks to higher energies in the EPI function reconstructed from the superconducting contribution.

D. In-based point contact

In the case of lead, the superconducting contribution to the spectrum associated with EPI is very large and, as can be seen in Fig. 7, its amplitude exceeds non-linearity in the normal state. Indium is intermediate in EPI

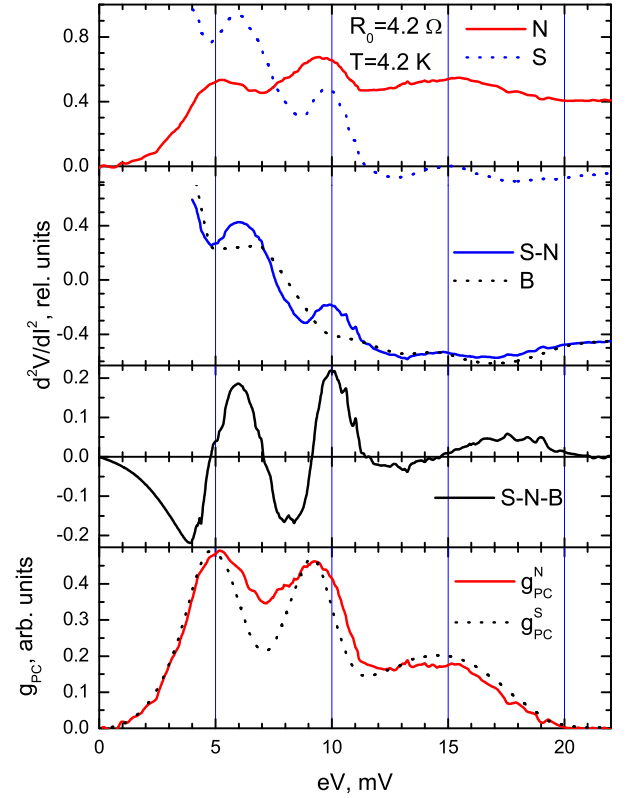


FIG. 9: EPI spectra of a $Pb - Sn$ point contact in the normal and superconducting states. Measurement temperature is above T_C of Sn ($T/T_C = 0.58$, $\Delta = 0.92\Delta_0$). Superconductivity is suppressed by a magnetic field (a). The difference between the superconducting and the normal spectra and the estimated background curve (b). Difference curve (after background subtraction) (c). Point-contact EPI function reconstructed through integrating the difference curve in panel (c) versus the EPI function of the normal state (d).

strength and, as follows from the table, exhibits a five-fold smaller elastic contribution to the spectrum compared to lead, but 2.7-fold higher than tin. At the same time, the superconducting transition temperature and the gap are only slightly ($\sim 8\%$) less than those of tin, so the inelastic contribution to the spectrum must be very close for these metals. Since, as noted above, the elastic and inelastic contributions counteract each other, in the case of indium they should, to a large extent, weaken each other. Fig. 10 shows the spectra of indium¹³. As can be seen in the figure, the contribution to the spectrum associated with superconductivity in indium is very small and of elastic nature. Unlike tin, where it was possible to restore the spectrum from the superconducting contribution in a wide temperature range (Figs. 3 and 4), for indium, this was possible only at the lowest temperature.

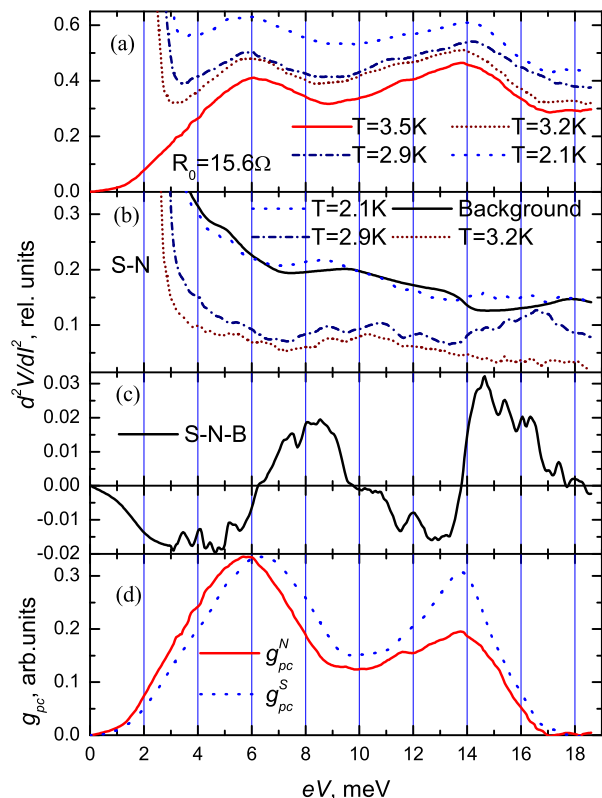


FIG. 10: EPI spectra of an In-In point contact in the normal and superconducting states at different temperatures (a). The differences between the superconducting and normal spectra, as well as the estimated background curve. $T = 2.1\text{K}$: $T/T_C = 0.62$, $\Delta = 0.89\Delta_0$; $T = 2.9\text{K}$: $T/T_C = 0.85$, $\Delta = 0.63\Delta_0$; $T = 3.2\text{K}$: $T/T_C = 0.94$, $\Delta = 0.41\Delta_0$ (b). Difference curve (after background subtraction) (c). Point-contact EPI function reconstructed by integrating the difference curve (c) versus the EPI function of the normal state (d).

IV. DISCUSSION

In determining the function of electron-phonon interaction, the traditional tunneling spectroscopy is limited to the superconductors with strong coupling. At the same time Yanson's point-contact spectroscopy focusses on metals in the normal state. Inelastic superconducting point-contact spectroscopy thus fills the gap and can be used to study superconductors with weak coupling. Moreover, as follows from the discussion of indium, the superconductors in which the elastic and inelastic contributions are close in value are the most complex objects since the elastic and inelastic contributions counteract each other, which leads to a weakening of the resulting contribution to the spectrum. When evaluating the sign and magnitude of the expected effect in such superconductors, first of all the transparency of the barrier between the electrodes should be taken into account. A situation is very likely to appear in which contacts with the different transparency of barriers exhibit different po-

sitions of the spectral maxima due to the predominance of elastic or inelastic spectral contributions. Note that it is not so much the magnitude of the elastic contribution to the spectrum as the ratio between the elastic and inelastic contributions that is important. For instance, as follows from the data in Table 1, the elastic contribution to the spectrum in MgB_2 is slightly larger than that in In. However, the resulting spectrum in MgB_2 is inelastic³. Here we should give attention to the magnitude of the superconducting gaps in In and MgB_2 . The inelastic contribution is proportional to the energy gap, which in MgB_2 is an order of magnitude larger than in In.

Even for superconductors with weak coupling there may be deviations from the theoretical predictions. For instance (see Table 1), the elastic contribution to the spectrum in Sn is greater than that in Ta by $\sim 12\%$. However, due to a shorter electron energy relaxation length, the presence of phonons with low group velocity results in a significant influence of the contact region on the formation of the superconducting contribution. As a result, sharpening of the phonon peaks and other deviations from the theoretical predictions are observed. Another typical example is 2H-NbSe_2 , a superconductor with covalent bonds between the atoms within the layer and van der Waals forces between the layers. Therefore, both the current spreading and dispersion of phonons in the point contacts based on NbSe_2 are anisotropic. This leads to a slower decrease of the concentration of nonequilibrium phonons with increasing the distance from the constriction, and thus, an increase of the superconducting contribution to the spectrum. As can be seen in Fig. 3 in Ref.³, this contribution is sufficiently large and only an order of magnitude smaller than the gap peculiarity in the spectrum.

To summarize, let us note that all of the observed deviations from the theoretical predictions are, in varying degrees, related to the influence of the contact region that requires further theoretical and experimental studies. Moreover, point contacts with a non-uniform distribution of impurities exhibiting diffusion transport through the junction and ballistic banks also require further studies. It should be noted that this situation is most easily achieved for superconductors with covalent bonds between atoms which have a rigid crystal lattice. For ordinary metals, due to their ductility, the lattice distortions upon forming point contacts could extend to the banks as well.

V. CONCLUSIONS

1. The EPI functions for Sn and Al were reconstructed from the superconductivity-related contributions to the spectra of point contacts based on these metals. The procedure of reconstruction of the EPI functions produces similar results across a wide range of temperatures. As follows from the theory of super-

conductors with weak coupling, the superconducting inelastic contribution to the spectrum manifests itself as *differential resistance maxima* in the first derivative of the excess current in the range of characteristic phonon energies. The position of these peaks coincides with the phonon peaks observed in the normal state of $S - c - S$ point contacts and, for $S - c - N$ point contacts, is shifted to *lower* energies by the value of the superconducting energy gap.

2. The EPI functions for Pb and In were reconstructed from the superconductivity-related contributions to

the spectra of point contacts based on these metals. For superconductors with strong coupling, the superconducting elastic contribution to the spectrum manifests itself as *differential conductivity maxima* in the first derivative of the excess current in the range of characteristic phonon energies. The position of these peaks *coincides* with the phonon peaks observed in the normal state of $S - c - N$ point contacts and, for $S - c - S$ point contacts, is *shifted to higher energies* by the value of the superconducting energy gap.

-
- ¹ Yu.G. Naidyuk and I.K. Yanson, Point-Contact Spectroscopy (Springer, New York, 2005).
 - ² A.V. Khotkevich and I.K. Yanson, Atlas of Point-Contact Spectra of Electron-Phonon Interaction in Metals (Kluwer Academic Publishers, Boston, 1995).
 - ³ N.L. Bobrov, V.V. Fisun, O.E. Kvitnitskaya, V.N. Chernobay, and I.K. Yanson, Fiz. Nizk. Temp. **38**, 480 (2012) [Low Temp. Phys. **38**, 373 (2012)].
 - ⁴ V.A. Khlus and A.N. Omel'yanchuk, Fiz. Nizk. Temp. **9**, 373 (1983) [Sov. J. Low Temp. Phys. **9**, 189 (1983)].
 - ⁵ V.A. Khlus, Fiz. Nizk. Temp. **9**, 985 (1983) [Sov. J. Low Temp. Phys. **9**, 510 (1983)].
 - ⁶ V.A. Khlus, Zh. Eksp. Teor. Fiz. **94**, 341 (1988) [Sov. Phys. JETP **66**, 1243 (1988)].
 - ⁷ I.O. Kulik, A.N. Omel'yanchuk, and R.I. Shekhter, Fiz. Nizk. Temp. **3**, 1543 (1977) [Sov. J. Low Temp. Phys. **3**, 740 (1977)].
 - ⁸ A.N. Omel'yanchuk, S.I. Beloborod'ko, and I.O. Kulik, Fiz. Nizk. Temp. **14**, 1142 (1988) [Sov. J. Low Temp. Phys. **14**, 630 (1988)].
 - ⁹ G.E. Blonder, M. Tinkham, and T.M. Klapwijk, Phys. Rev. B **25**, 4515 (1982).
 - ¹⁰ Principles of Electronic Tunneling Spectroscopy, edited by E.L. Wolf (Oxford University Press, 1985).
 - ¹¹ J.M. Rowell and W.L. McMillan, Phys. Rev. Lett. **14**, 108 (1985).
 - ¹² I.K. Yanson, G.V. Kamarchuk, and A.V. Khotkevitch, Fiz. Nizk. Temp. **10**, 423 (1984) [Sov. J. Low Temp. Phys. **10**, 220 (1984)].
 - ¹³ G.V. Kamarchuk and A.V. Khotkevitch, Fiz. Nizk. Temp. **13**, 1275 (1987) [Sov. J. Low Temp. Phys. **13**, 717 (1987)].
 - ¹⁴ P.N. Chubov, I.K. Yanson, and A.I. Akimenko, Fiz. Nizk. Temp. **8**, 64 (1982) [Sov. J. Low Temp. Phys. **8**, 32 (1982)].
 - ¹⁵ A.V. Khotkevitch, V.V. Khotkevitch, I. K. Yanson, and G. V. Kamarchuk, Fiz. Nizk. Temp. **16**, 1199 (1990) [Sov. J. Low Temp. Phys. **16**, 693 (1990)].
 - ¹⁶ J.M. Rowell, W.L. McMillan, and C.R. Dynes, A Tabulation of Electron-Phonon Interaction in Superconducting Metals and Alloys, Part 1 (Murray Hill, New Jersey, USA, 1973) (Preprint/Bell Labs).
 - ¹⁷ G.V. Kamarchuk, A.V. Khotkevitch, and I.K. Yanson, Fiz. Tverd. Tela **28**, 455 (1986) [Sov. Phys. Solid State **28**, 254 (1986)].